Metabolic alterations provide insights into Stylosanthes roots responding to phosphorus deficiency

Jiajia Luo
Hainan University https://orcid.org/0000-0002-8488-1911
Yunxi Liu
Hainan University
Huikai Zhang
Hainan University
Jinpeng Wang
Hainan University
Zhijian Chen
Hainan University
Lijuan Luo
Hainan University
Guodao Liu
Hainan University
Pandao Liu (liupandao2019@163.com)

Research article

Keywords: Metabolome, Stylosanthes, Phosphorus deficiency, Root morphology, Flavonoid, Expansin

Posted Date: October 18th, 2019

DOI: https://doi.org/10.21203/rs.2.13121/v2

Version of Record: A version of this preprint was published on February 22nd, 2020. See the published version at https://doi.org/10.1186/s12870-020-2283-z.

Abstract

Background: Phosphorus (P) deficiency is one of the major constraints limiting plant growth, especially in acid soils. Stylosanthes (stylo) is a pioneer tropical legume with excellent adaptability to low P stress, but its underlying mechanisms remain largely unknown. Results: In this study, the physiological, molecular and metabolic changes in stylo responding to phosphate (Pi) starvation were investigated. Under low P condition, the root growth in stylo was significantly enhanced, which was accompanied with up-regulation of expansin genes participating in cell wall loosening. Metabolic profiling analysis showed that a total of 256 metabolites with differential accumulation were identified in stylo roots responding to P deficiency, which mainly include flavonoids, sugars, nucleotides, amino acids, phenylpropanoids and phenylamides. P deficiency led to significant reduction in the accumulation of phosphorylated metabolites (e.g., P-containing sugars, nucleotides and cholines), suggesting that internal P utilization was enhanced in stylo roots. However, flavonoid metabolites, such as kaempferol, daidzein and their glycoside derivatives, were significantly increased in P-deficient stylo roots. Furthermore, the transcripts of various genes involved in flavonoids synthesis were found to be up-regulated by Pi starvation in stylo roots. In addition, the abundance of phenolic acids and phenylamides was significantly increased in stylo roots during P deficiency. The enhanced accumulation of the metabolites in stylo roots, such as flavonoids, phenolic acids and phenylamides, might facilitate P solubilization and cooperate with beneficial microorganisms in rhizosphere, and thus contributing to P acquisition and utilization in stylo. Conclusions: These results suggest that stylo plants cope with P deficiency by modulating root morphology, scavenging internal Pi from phosphorylated metabolites and enhancing accumulation of flavonoids, phenolic acids and phenylamides. This study provides valuable insights into the complex responses and adaptive mechanisms of stylo to P deficiency.

Background

Phosphorus (P) is one of the essential macronutrients for plant growth. It involves in plant photosynthesis, energy conversion, signal transduction and biomacromolecule biosynthesis [1]. Soluble inorganic phosphate (Pi) is the major form of P that can be directly utilized by plants from soils [2]. However, P is easily fixed by organic compounds, iron (Fe) or aluminum (Al) oxides in soils [3]. Low Pi availability is a major constraint limiting crop growth and yield [4]. In modern agriculture, Pi-fertilizers are excessively applied to alleviate P deficiency [5]. Excessive application of Pi fertilizers is not favored economically and environmentally [6]. Therefore, to maintain the sustainable development of agriculture, it is important to understand how plants adaptation to Pi starvation, which can gain knowledge to breed cultivars with high P efficiency [7].

Plants have evolved a series of adaptive mechanisms to enhance P acquisition efficiency (PAE) and P utilization efficiency (PUE) in Pi-limited soils [8]. The major adaptive strategies of increasing PAE include modification of root architecture and morphology [9], exudation of organic acids from root to rhizosphere [10], secretion of phosphatases and ribonucleases [11], enhancing the expression of Pi transporter [12] and symbiosis with arbuscular mycorrhiza (AM) or other plant growth-promoting rhizobacteria (PGPR)

[13]. The major PUE-related strategies include replacement of membrane phospholipids by galactolipids and sulfolipids [14], remobilization Pi from the vacuolar P storage [15], and alternative metabolic bypass reactions that depend on inorganic pyrophosphate (PPi) instead of Pi [16]. These complex responses can be achieved by the coordination of an elaborate P signaling network [17, 18]. Over the past few decades, several key regulators involved in this network have been functionally characterized, such as PHR1 (phosphate starvation response 1), SPX domain-containing proteins, PHO2 (a ubiquitin-conjugating E2 enzyme) and microRNA399 [19-21].

Low Pi availability induces dramatic changes in gene and protein expressions in plants [22, 23]. Transcriptomic and proteomic analyses have been widely used to investigate Pi starvation response (PSR) genes and proteins in various plant species, such as *Arabidopsis thaliana* [24], rice (*Oryza sativa*) [25, 26], maize (*Zea mays*) [27-30] and masson pine *(Pinus massoniana*) [30, 31]. A 3group of PSR genes and proteins have been implicated in P uptake, P reallocation, P-containing metabolites catabolism, organic acid metabolism, signal regulating, cell wall synthesis and modification [32]. For example, expansins are superfamily proteins that modify cell wall loosening, leading to cell extension [33]. *GmEXLB1*, one of Pi starvation-inducible expansin genes, identified by transcriptome profiles in soybean (*Glycine max*), has been characterized involved in P acquisition by regulating root growth [34]. Recently, a pair of rice vacuolar Pi efflux transporters (OsVPE1 and OsVPE2) identified by vacuolar membrane proteomics, have been demonstrated to participate in vacuoles Pi remobilization [35]. Although the molecular properties of several PSR genes and proteins have been well illuminated, biological functions of vast PSR genes and proteins have not been documented.

Along with the changes in gene and protein expressions, metabolic alterations also occur in P-deficient plants. Metabolomic analysis using gas or liquid chromatography mass spectrometry (GC-MS and LC-MS) techniques is considered as one of the useful tools in investigating metabolism mechanisms of plants adaptation to Pi starvation [36]. Metabolites profiling studies have been carried out in several plants response to P deficiency, such as Arabidopsis [37], rice [38], maize [39], barley (*Hordeum vulgare*) [40], wheat (*Triticum aestivum*) [41], soybean [42] and tea (*Camellia sinensis*) [43]. Furthermore, a part of metabolites differentially regulated by Pi starvation are conserved in different plants. For example, decreasing in the concentrations of phosphorylated sugars is generally observed in P-deficient plants. However, significant variations in changes of several amino acids have been found across or within plant species. Furthermore, flavonoids belong to the large family of phenylpropanoid metabolites, which are involved in plant growth, development and plant-environment interactions [44]. Through metabolome profiling, the effects of P deficiency on the levels of flavonoids have been analyzed only in a few plant species, including Arabidopsis [37], soybean [42] and tea [43]. However, thousands of flavonoids have been identified in various plant species [44]. The response of diverse flavonoids to low P stress is still unclear in plants.

Stylo (*Stylosanthes* spp.) is an important forage legume and cover crop in tropical and subtropical areas, with excellent adaptability to acid soils [45]. P deficiency, along with Al and manganese (Mn) toxicity, are considered as major limiting factors for crop growth and production in acid soils [46]. Therefore, it is

possible that stylo is capable of overcoming these constraints with potential adaptive mechanisms. Transcriptomics or proteomics profiling has been used to analyze the responses of stylo to Al and Mn toxicity [47-49]. However, only a little is known about how P deficiency affects molecular profiling in stylo. In this study, changes in growth performance, PSR genes expression and metabolome profiling in response to Pi starvation were investigated in stylo roots.

Results

Physiological responses of stylo under Pi starvation

To assess the dynamic alternations of stylo under P-sufficient (+Pi) and P-deficient (-Pi) conditions, a time-course of hydroponic cultivation experiment was performed. Results showed that the inhibition on the shoot dry weight was observed after 7 d of -Pi treatments, and the difference between -Pi and +Pi became increasing significantly as the treatment time increased (Fig. 1). In contrast, no difference in root dry weight was found between -Pi and +Pi treatments for 7 d. However, root dry weight was increased by 40.3 and 31.2% after 10 and 15 d of -Pi treatment, respectively (Fig. 1a, b; Additional file 1: Fig. S1). Consistently, the total root length, root surface area and root volume were increased after 10 and 15 d of Pi starvation (Fig. 1c, d, e). The maximum ratio of total root length and root surface area under -Pi versus +Pi treatments was observed at 15 d of treatments. The ratio of total root length and root surface was increased by 44.6 and 56.1%, respectively (Additional file 1: Fig. S2).

The ratio of root/shoot was also influenced by Pi availability, as reflected by a significant increase in ratio of root/shoot under Pi starvation. Furthermore, the maximum ratio of root/shoot was reached at 15 d of -Pi treatment, which was 2.6-fold higher than that of +Pi treatment (Additional file 1: Fig. S3). Additionally, after 15 d of -Pi treatment, total P content was declined, whereas the activity of root acid phosphatase (APase) and phenylalanine ammonia (PAL) were increased by 209.0% and 100.5%, respectively. Root total phenol, flavonoid, total antioxidant capacity (T-AOC) were also increased by -Pi treatment compared to 15 d of +Pi treatment (Additional file 1: Fig. S4). These results suggest that a series of morphological and physiological changes are occurred in stylo under Pi starvation.

Characterization of *expansin* gene family in stylo roots

Expansin protein family, located in the cell wall, is associated with regulating plant root morphology and architecture [50]. A total of 16 stylo *expansin* genes were identified in stylo (Additional file 2: Table S1). Phylogenetic analysis showed that 16 stylo *expansin* members were divided into four subfamilies, including 9 *SgEXPA*, 1 *SgEXLA*, 3 *SgEXPB* and 3 *SgEXLB* (Additional file 1: Fig. S5). The expression patterns of these genes were further analyzed in roots of stylo with 15 d of P treatments. Results showed that 4 out of 9 *SgEXPAs*, *SgEXPB2* and *SgEXLB1* were up-regulated, whereas *SgEXLB3* was down-regulated by Pi starvation. The expressions of the remaining stylo *expansin* genes were not affected by low Pi availability (Fig. 2). These results suggest that stylo *expansin* genes participate in modifying root morphology under low P condition.

Overview of metabolome in stylo roots response to Pi starvation

To evaluate metabolic responses to Pi starvation, an LC-MS/MS analysis was performed on stylo roots at two P treatments for 15 d. A total of 708 metabolites were identified under two P levels (Additional file 3: Table S2). Principal component analysis (PCA) showed that principal component one (PC1) nicely defined the difference between +Pi (triangles) and -Pi (circles) plant material, which represented about 80.15% of the variation. The intragroups of three biological repeats of +Pi and -Pi treatments were similar to each other on the PC1, suggesting a good reproducibility of the data (Fig. 3a). The metabolites with the ratio of -Pi/+Pi ≥ 2 or ≤ 0.5 and the variable importance in project (VIP) ≥ 1 were considered as differentially accumulated metabolites (DAMs). A total of 256 DAMs were identified in stylo roots at two P treatments, including 136 low P up-regulated metabolites and 120 down-regulated metabolites (Fig. 3b). In the heatmap, the DAMs were clustered in two branches: the down-regulation cluster (color in blue) and up-regulation cluster (color in red). The root samples were also clustered into +Pi and -Pi treatment branches (Additional file 1: Fig. S6). All of the identified 256 DAMs were classified into 14 categories, including flavonoids, phenylpropanoids, phenylamides and its derivatives, amino acids and cholines, the up-regulated numbers of which were higher than that of the down-regulated. However, the numbers of up-regulated amino acid derivatives and sugars were less than that of the down-regulated (Fig. 3c).

Changes of sugars, cholines, nucleotide and its derivatives in stylo roots response to Pi starvation

Based on the existence of phosphate group in metabolites, sugars, cholines, nucleotide and its derivates were classified into P-containing and non-P-containing two groups. For the 13 DAMs belonged to sugars, the relative levels of 6 P-containing sugars were declined by-Pi treatment. Among them, 2-deoxyribose 1-phosphate, ribulose-5-phosphate, mannose-6-phosphate and fructose-1-phosphate were decreased more than 10-fold in the -Pi treatment compared to those of in the +Pi treatment. In contrast, the relative levels of 3 non-P-containing sugars were significantly increased, including glucose, inositol and gluconic acid (Fig. 4). The relative levels of 4 non-P-containing cholines were increased. The levels of P-containing cholines, such as glycerol-3-phosphocholine (GPC) and phosphocholine (PCho), were decreased by 58.43- and 20.96-fold in the -Pi treatment compared to those of in the -Pi treatment, respectively.

In addition, 28 DAMs were identified as nucleotide and its derivates. Among them, 10 out of 14 non-P-containing nucleotides were increased, while 11 out of 14 P-containing nucleotides were decreased in stylo roots exposed to low P stress. Nicotinic acid mononucleotide, cytidylic acid, uridine 5'-diphospho-D-glucose, uridine 5'-monophosphate, nicotinic acid adenine dinucleotide and adenosine monophosphate were declined more than 10-fold.

To detect the response of hydrolases participating in P-containing metabolites catabolism to low Pi stress, the expressions of 5 stylo purple acid phosphatase (*PAP*) and 3 ribonuclease (*RNS*) genes were analyzed by quantitative real-time polymerase chain reaction (qRT-PCR). Result showed that the expressions of 4 out of 5 *SgPAPs* were up-regulated by-Pi treatment, especially for *SgPAP10/12/23*. The expressions of 3 out of 4 *SgRNSs* were enhanced under low Pi stress.

Alterations of amino acid and its derivatives in stylo roots response to P deficiency

Among the identified amino acids, 9 out of 22 were considered as DAMs (Additional file 4: Table S3), and 7 out of 9 DAMs were significantly induced under -Pi treatment, whereas glutamate (Glu) and cystine (Cys) were decreased by Pi starvation in stylo roots. Citrulline was the amino acid with the highest induction (more than 5-fold) (Fig. 5). In addition, 81 amino acid derivatives were also identified in metabolome. Among them, 29 amino acid derivatives were DAMs, including 9 up-regulated and 20 down-regulated amino acid derivatives (Additional file 4: Table S3; Fig. 5).

Analysis of flavonoids in stylo roots response to P deficiency

A total of 54 DAMs belonged to flavonoids, including 23 flavonoes, 16 flavonols, 6 flavanones, 4 isoflavanes, 2 flavanols, 2 anthocyains and 1 chalcone. The accumulation of a larger number of flavonoids was increased in stylo roots under low P stress (Fig. 6a).

For the differentially accumulated flavones, the relative levels of 19 out of 23 flavones were significantly increased, including 4 glycoside derivatives of apigenin and 4 glycoside derivatives of chrysoeriol, while the remaining flavones were declined by -Pi treatment (Fig. 6b; Fig. 7).

For the differentially accumulated flavonols, the relative levels of 9 out of 16 flavonols were increased, whereas the levels of 7 flavonols were decreased under -Pi stress. Although the relative levels of kaempferol and quercetin were increased after Pi starvation, their glycoside derivatives displayed different responses to low P stress. Three glycoside derivatives of kaempferol were up-regulated, whereas 5 glycoside derivatives of quercetin were down-regulated (Fig. 6b; Fig. 7).

For the differentially accumulated flavanones, the abundance of most flavanones was increased in stylo roots under low P stress, except hesperetin O-hexoside. The flavanone with the strongest induction was liquiritigenin, which was up to 4.97-fold (Fig. 6b; Fig. 7). Similarly, the concentrations of 4 isoflavones were increased under -Pi stress. Three of them (rotenone, daidzein and daidzein 7-O-glucoside) were increased more than 5-fold (Fig. 6b).

Subsequently, the expressions of stylo *2-hydroxyisoflavanone dehydratase* (*SgHID*) and *uridine diphosphate glycosyltransferase* (*SgUGT*) involved in daidzein and daidzein 7-O-glucoside synthesis were further analyzed. Results showed that 3 out of 5 *SgHIDs* and 2 out of 3 *SgUGTs* were significantly up regulated by low P stress (Fig. 8). In addition, the expression of stylo *flavonoid 3'-hydroxylase* (*SgF3'H-1*), *flavonol synthase* (*SgFLS-1*) and *flavanone 3-hydroxylase* (*SgF3H-1*) encoding enzymes involved in flavonoids synthesis were detected (Fig. 7). Results showed that the expression of *SgF3'H-1*, *SgFLS-1* and *SgF3H-1* were up-regulated under P deficient condition (Fig. 8).

Analysis of phenylpropanoids, phenylamides and its derivatives in stylo roots response to P deficiency

In addition to flavonoids, other differentially accumulated phenylpropanoids were also identified in metabolome, including 7 phenolic acids and 8 non-phenolic acid phenylpropanoids. For phenolic acids,

the concentrations of 5 DAMs were significantly increased, especial for, caftaric acid, which was increased more than 10-fold under -Pi treatment. For non-phenolic acid phenylpropanoids, the concentrations of 5 DAMs were enhanced, whereas 3 DAMs were decreased. Among the increased DAMs, the relative level of sesamin was increased more than 10-fold.

Fifteen differentially accumulated phenylamides and its derivatives were identified in the metabolome, including 13 up-regulated and 2 down-regulated DAMs (Fig. 9). The relative levels of 3 phenylamides (N-benzoyl-tryptamine, N-feruloyl-cadaverine and N-feruloyl-putrescine) were increased more than 5-fold. As shown in Fig. 10, numerous metabolites in phenylpropanoids metabolic pathway were up-regulated by P deficiency. Interestingly, all ρ-coumaric acid and four corresponding derivatives were increased in stylo roots in response to Pi starvation. These results indicate that the induction of phenylpropanoids and phenylamides may be the adaptive mechanism of stylo in response to low P stress.

Discussion

Modification of stylo root morphology in response to low Pi availability

As the major organ for Pi uptake, root is of high plasticity in its developmental response to low Pi availability [51]. Cumulative studies show that plant adaptation to P deficiency includes the changes in root architecture and morphology, such as promotion of lateral root growth, enhancement of root hair development, and even formation cluster roots in Proteaceae plants [4]. Such developmental strategies increase the root-soil contact surface, and thus facilitating exploitation of Pi reserves from soils [9]. In this study, root dry weight, root length, root surface area and root volume were significantly increased in stylo under low P treatment for 10 d and 15 d, suggesting that stylo adapts to P deficiency through modification of root growth (Fig. 1).

Cell wall loosening is one of vital progress in root modification, which is mediated by expansin superfamily [33]. Expansins consist of four subfamilies, including α-expansin (EXPA), expansin-like A (EXLA), β-expansin (EXPB) and expansin-like B (EXLB) [52]. To data, three expansin members in plants have been demonstrated to function in the adaptation to P deficiency by regulating root architecture and morphology, including *TaEXPB23* from wheat [53], *GmEXPB2* and *GmEXLB1* from soybean [34, 54]. In this study, *SgEXPB2* and *SgEXLB1*, the homologous genes of *GmEXPB2* and *GmEXLB1* in stylo, were up-regulated by Pi starvation in roots (Fig. 2; Additional file 1: Fig. S5). Furthermore, the expressions of 4 *SgEXPAs* belong to *EXPA* subfamily, were also increased under low P stress (Fig. 2; Additional file 1: Fig. S5). These results suggest that *expansin* genes play a role in the modifications of root morphology in responses to P deficiency in stylo.

Accumulation of glucose in P-deficient stylo roots

When subjected to P deficiency, plants usually alter the allocation of carbohydrates. More carbohydrates are allocated to the root system, stimulating root growth and resulting in the increase their root/shoot ratio [55]. In this study, root/shoot ratio in stylo was significantly increased by P deficiency, accompanied

by stimulation of root growth (Fig. 1; Additional file 1: Fig. S3). Metabolomic analysis showed that the concentration of glucose increased more than 10-fold in P-deficient stylo roots (Fig. 4). Similarly, accumulations of glucose are observed in tea and ryegrass (*Lolium perenne*) under low Pi condition [43, 56]. Glucose, one of the carbohydrates from photosynthesis, is not only involved in plant energy supply, carbon metabolism and cell wall synthesis, but also emerged as a crucial signaling molecule [57]. Recently, glucose signaling has been shown to facilitate root growth and development by interacting with phytohormones [58]. In Arabidopsis, several studies demonstrate that glucose crosstalk with auxin signaling displays positive functions in facilitating cell expansion and lateral root formation [58]. These results suggest an important role of the glucose in plants adaptation to P deficiency. Glucose possible function as both energy and signaling molecules for regulating root growth in stylo.

Scavenging of Pi from P-containing metabolites during P deficiency

Remobilization of P-containing metabolites is considered as an important strategy for plants adaption to P deficiency [15]. Under P-limiting conditions, P-containing metabolites, such as nucleic acid, phospholipids and phosphorylated sugars, can be scavenged to maintain Pi homeostasis in plant cells [59]. Metabolomic analysis shows that phosphorylated sugars are significantly reduced by P deficiency in various plants, such as Arabidopsis [37], barley [40], white lupin (*Lupinus albus*) [60] and *Populus cathayana* [61]. Similarly, the accumulation of 6 phosphorylated sugars were significantly decreased in P-deficient stylo roots (Fig. 4). Furthermore, Pi starvation resulted in decreased concentrations of 2 P-containing cholines and 11 P-containing nucleotides (Fig. 4). These results suggest that widespread alterations in P-containing metabolites occur in stylo roots response to Pi starvation. There were further supported by the observation that a set of genes (4 *SgPAPs* and 3 *SgRNSs*) involved in the degradation of P-containing metabolites were up-regulated by Pi starvation in stylo roots (Additional file 1: Fig. S7).

P deficiency enhances the levels of flavonoids in stylo roots

Flavonoids, one of the pivotal secondary metabolites, play diverse biological roles in plants, such as transport of auxin, modulation of reactive oxygen species, protection against ultraviolet-B, and interaction with rhizosphere microorganisms [44]. So far, more than 10,000 structural variants of flavonoids have been identified in plants. Based on their basal structures, flavonoids could be divided into flavones, flavanones, flavonols, isoflavones, flavanols, anthocyanins and chalcones [62]. Among them, flavonols (e.g., quercetin, kaempferol, isorhamnetin and kaempferol glycosides) have been reported accumulated in Arabidopsis during Pi starvation [37, 64]. In this study, 41 out of 54 differentially accumulated flavonoids were up-regulated by Pi starvation in stylo roots (Fig. 3c; Fig. 6). The concentrations of kaempferol and its glycoside derivatives belonged to flavonols were significantly enhanced under low Pi condition (Fig. 6b). Consistently, S*gFLS-1*, participating in the last step of kaempferol biosynthesis, was up-regulated by Pi starvation in stylo roots (Fig. 7, 8). It has been reported that plant roots can release kaempferol to promote Fe availability by solubilizing Fe complex in soils [44]. Protocatechuic acid, the other flavonoids belong to flavanols derivatives, plays a similar function with kaempferol, involving in Fe solubilization in rice during Fe deficiency [64]. In this study, the concentrations of protocatechuic acid and its derivative

(protocatechuic acid O-hexoside) dramatically increased in stylo roots under low Pi condition (Fig. 6b). It is well known that Fe and P can form insoluble complexes in soils. Along with the Fe mobilization by flavonoids, Pi can be released. Therefore, the accumulation of kaempferol and protocatechuic acid in stylo roots might facilitate mobilization of insoluble P.

It has been reported that the levels of isoflavones (e.g., daidzein) are increased in P-deficient bean (*Phaseolus vulgaris*) [65]. Similarly, the accumulation of daidzein and daizein 7-O-glucoside was enhanced by more than 5-fold in stylo under low Pi condition (Fig. 6b). Consistently, a set of genes (*SgUGTs* and *SgHIDs*) involved in daidzein and daizein 7-O-glucoside biosynthesis, were found to be up-regulated by Pi starvation in stylo roots (Fig. 8). It has been demonstrated that daidzein play vital roles in symbiotic network formation with AM fungi, contributing to Pi uptake in soybean roots [62]. In addition, delphinidin 3-glucoside and peonidin 3-glucoside belonged to anthocyanins, were significantly increased by P deficiency in stylo roots. It has been suggested that the accumulated anthocyanins in plant shoots and leaves could have a photoprotective function, but the functions of anthocyanins in roots remain to be clarified [42].

Increased accumulation of phenolic acids and phenylamides in P-deficient stylo roots

Except for flavonoids, the other class of secondary metabolites, a set of phenolic acids were also increased in P-deficient stylo roots. For example, the concentration of caftaric acid was enhanced by more than 10-fold under Pi starvation (Fig. 9). It has been reported that phenolic acids exuded from roots can promote mobilization of insoluble P complexes (Fe-P and Al-P), and thus enhancing Pi availability. [66, 67]. Moreover, it has been clarified that caftaric acid positively contribute to the interaction of AM fungi with plants [68].

Phenylamides, also referred to as hydroxycinnamic acid amides (HCAA) or phenolamides, are synthesized from phenolic acid derivatives and polyamines. It has been reported that phenylamides play important roles in protecting plants against abiotic and biotic stresses [69, 70]. However, responses of phenylamides to P deficiency are not clear. In stylo roots, 15 differentially accumulated phenylamides were identified (Fig. 9). Among them, the accumulation of 13 phenylamides was increased in response to P deficiency, such as N-feruloyl-putrescine (Fig. 9). Recently, N-feruloyl-putrescine has been demonstrated to participate in the interaction with PGPR in rice roots [70]. Therefore, P-deficiency leads to accumulation of flavonoids, phenolic acids and phenylamides, which might facilitate to Pi remobilization and cooperate with beneficial microorganisms (e.g., AM fungi and PGPR) in stylo.

Conclusions

This study demonstrated that stylo root morphology were modified by P deficiency, including a wide range of physiological, molecular and metabolic modulations. Under low Pi condition, the enhancement of root growth and *expansin* gene expression can improve Pi acquisition in stylo. P deficiency led to decreases in P-containing metabolites, suggesting that internal Pi utilization was enhanced in stylo roots. Furthermore, the accumulation of flavonoids, phenolic acids and phenylamides were increased in P-

deficient stylo roots, which might contribute to plant-environment interactions. Taken together, this study provides a comprehensive understanding of complex responses and diverse adaptations to Pi starvation in stylo roots.

Methods

Plant growth and treatment

In this study, stylo genotype 'TF0291' was used., which was originally introduced to Chinese Academy of Tropical Agriculture Sciences (CATAS) from International Center for Tropical Agriculture (CIAT) in Colombia. The seeds of stylo TF0291 were provided by the Tropical Pasture Research Center, Institute of Tropical Crop Genetic Resources, CATAS, Hainan Province, China.

Stylo seeds were pre-germinated on wet filter paper at 28°C. After germinated for 3 d, the uniform seedlings were transferred to blue plastic pots filled with modified Magnavaca's nutrient solution according to Famoso et al. [71], containing KCl (1 mmol L^{-1}), $CaCl_2$ (1 mmol L^{-1}), Fe-EDTA (77 μmol L^{-1}), $MgSO_4$ (200 μmol L^{-1}), $Mg(NO_3)_2$ (500 μmol L^{-1}), NH_4NO_3 (1.5 mmol L^{-1}), $MnCl_2{\cdot}4H_2O$ (11.8 μmol L^{-1}), $ZnSO{\cdot}7H_2O$ (3.06 μmol L^{-1}), $CuSO_4{\cdot}5H_2O$ (0.8 μmol L^{-1}), H_3BO_3 (33 μmol L^{-1}), $Na_2MoO{\cdot}4H_2O$ (1.07 μmol L^{-1}), $MgCl_2{\cdot}6H_2O$ (155 μmol L^{-1}), KH_2PO_4 (250 μmol L^{-1}). The plants were grown in a greenhouse at Hainan University, China (E121°54', N30°52') under a natural day-night cycle and environment. After 7 d, the seedlings were transferred to fresh modified Magnavaca's nutrient solution supplied with (+Pi) or without (-Pi) 250 μmol/L KH_2PO_4. After 0, 7, 10, 15, 20 d of P treatments, root and shoot were harvested for determination of dry weight, total P content, total root length, root surface area and root volume. Roots with different P treatments for 15 d were harvested and stored in -80°C for subsequent metabolite and qRT-PCR analysis.

Assessment of root parameters, total P content, APase activity and other biochemical parameters

To determine root parameters (root length, surface area, volume), stylo roots were scanned at 400 dpi by a scanner (Epson, Japan). Scanned images were further analyzed through WinRHIZO program (2009, Regent, Canada).

After dry weight determination, total P content in shoot and root were measured using the phosphorus-molybdate blue color reaction method according to Murphy and Riley [72]. A standard curve was used for calculating the P content. APase activity in stylo roots with different P treatments was measured according to Liu et al. [73]. APase activity was measured by detecting the production of ρ-nitrophenol at absorbance of 405 nm.

T-AOC and PAL activity were detected as described by Qiao et al. [74] using the commercial chemical assay kits (Nanjing Jiancheng Bioengineering Institute, Nanjing, China). Briefly, T-AOC activity was determined based on ferric reduced/antioxidant reaction system, which Fe^{3+}-tripyridine triacridine (TPTZ)

was reduced to F^{2+}-TPTZ by addition of reductive substance. F^{2+}-TPTZ was detected at absorbance of 520 nm. The produce rate of F^{2+}-TPTZ was used to calculate T-AOC activity. To assay PAL activity, the cinnamic acid produce rate was tested by spectrophotometry at absorbance of 290 nm (Code: A137-1-1). Protein content in the samples was determined based on the Coomassie Brilliant Blue method [75]. Total phenols and flavonoids content were detected using the commercial chemical assay kits (Jiancheng Bioengineering Institute, Nanjing, China). For total phenols content determination, as phenolic substances can be reduced from molybdic acid to generate blue compounds under alkaline condition, total phenols content was detected at absorbance of 760 nm according to the concentration of blue compounds. For flavonoids content determination, as flavonoids and aluminum ions can be reacted to form red compounds in alkaline nitrite solution, total flavonoids content was detected at absorbance of 502 nm according to the concentration of red compounds.

Metabolite analysis

The metabolomic analysis was conducted at MetWare Biotechnology Limited Company (Wuhan, China). All six root samples (three biological repetitions for +Pi and -Pi groups) were used. Metabolites were evaluated through untargeted LC-MS/MS technology. Extraction and metabolite analysis were performed as described by Chen et al. [76]. Briefly, root samples were crushed into fine powder using grinding mill (MM 400, Retsch), 100 mg samples were extracted in 1.0 mL 70% aqueous methanol overnight at 4°C. Supernatant components were collected and filtered with a 0.22 μm micropore filter (SCAA-104, ANPEL, Shanghai, China) centrifuged at 10,000 g for 10 min before LC-MS/MS analysis.

Two μL of each sample was injected into an Ultra Performance Liquid Chromatography (UPLC, Shim-pack UFLC SHIMADZU CBM30A) equipped with a tandem mass spectrometry (MS/MS, Applied Biosystems 6500 Q TRAP). In UPLC, samples were separated with a reverse-phase Waters Acquity UPLC HSS T3 C18 column (1.8 μm, 2.1 mm × 100mm). The mobile phase contained eluent A (0.04% acetic acid in aqueous solution) and B (0.04% acetic acid in acetonitrile solution). The gradient of separation program was set at 95:5 (A:B, v/v) at 0 min, 5:95 (A:B, v/v) at 11.0 and 12.0 min, 95:5 (A:B, v/v) at 12.1 and 15.0 min. The flow rate and column temperature were maintained at 0.4 ml/min and 40°C, respectively. For MS/MS, electrospray ionization (ESI) source operation parameters were set as follows: positive ion mode was used in the instrument; ion source was turbo spray; source temperature was set to 550°C; ion spray voltage was adjusted to 5.5 kV; the ion source gas I, gas II, curtain gas were set at 55, 60, 25 pounds per square inch, respectively. For triple quadrupole (QQQ) scans, each ion pair was scanned according to the optimized declustering potential and collision energy as multiple reaction monitoring (MRM) experiments.

The qualitative and quantitative analysis of metabolites were conducted according to the previous study [77]. The quantitation of metabolites was performed by matching the secondary spectral information with self-built MetWare database (MWDB) and public database of metabolite information. The quantitation of metabolites was analyzed through MRM of QQQ MS/MS. In addition, DAMs were

identified by orthogonal projection to latent structure-discriminant analysis (OPLS-DA), according to the criteria of fold change (-Pi/+Pi) ≥ 2 or ≤ 0.5, and the variable importance in project (VIP) ≥ 1 [78].

Quantitative real-time PCR (qRT-PCR) analysis

Total RNA was extracted using the RNA-solve reagent (Omega Biotech, USA). First strand cDNA synthesis from DNase I-treated total RNA was performed by M-MLV reverse transcriptase (Promega, Madison, WI, USA). qRT-PCR was carried out using SYBR Premix Ex Taq II (Takara, Japan) on the Rotor-Gene 3000 qRT-PCR system (Corbett Research, Australia). To reveal the relative levels of candidate genes response to Pi-starvation, which were related to the modification of plant cell wall, the gradation of P-containing metabolites, and synthetic of possible key flavonoid metabolites, based on the ribonucleic acid sequencing (RNA-Seq) data from NCBI database (PRJNA431518, SRX6928121), the expressions of the following genes were detected: *expansin* gene, *SgPAP*, *SgRNS*, *SgF3'H*, *SgFLS*, *Sg F3H*, *SgHID*, *SgUGT*. The housekeeping gene, *elongation factor 1-alpha* (*SgEF-1α*, accession number: JX164254), was used to normalize gene expression. The primers of genes for qRT-PCR analysis and gene accession numbers were listed in Additional file 2: Table S1. Four biological replicates were included in this study, and the relative expression levels were calculated according to Liu et al. [79]. In addition, multiple sequence alignments and phylogenetic tress of stylo *expansin* family genes were constructed using Clustal X and MEGA 5, respectively.

Statistical analysis and visualization

The means and standard errors of dry weight, total P content, root parameters, physiological indicators and gene expressions were analyzed by Excel 2016 (Microsoft Corporation, Redmond, WA, USA). One-way analysis of variance (ANOVA) with least significant difference (LSD), Duncan and Student's *t*-test were performed using SPSS (Version 19.0, IBM, Chicago, IL, USA) software. PCA, volcano diagram, clustered heatmap and circular figures were conducted in program R (v 3.5.1). Before analysis, the raw data was Z score-transformed for normalization in heatmap. The metabolic category figure was created with Microsoft Excel 2016. Metabolic pathways were constructed according to pathway analysis in the Kyoto Encyclopedia of Genes and Genomes (KEGG) metabolic database (http://www.kegg.jp/). To determine the metabolic change folds, untransformed mean values (n = 3) were employed to calculate -Pi/+Pi ratios.

List Of Abbreviations

Al: Aluminum; AM: Arbuscular mycorrhiza; ANOVA: One-way analysis of variance; APase: Acid phosphatase; CATAS: Chinese Academy of Tropical Agriculture Sciences; CIAT: International Center for Tropical Agriculture; Cys: Cystine; DAMs: Differentially accumulated metabolites; EF-1α: Elongation factor 1-alpha; ESI: Electrospray ionization; F3'H: Flavonoid 3'-hydroxylase; F3H: Flavanone 3-hydroxylase; Fe: Iron; FLS: Flavonol synthase; GC-MS: Gas chromatography mass spectrometry; Glu: Glutamate; GPC: Glycerol-3-phosphocholine;HCAA: Hydroxycinnamic acid amides; HID: 2-hydroxyisoflavanone dehydratase; KEGG: Kyoto Encyclopedia of Genes and Genomes; LC-MS: Liquid chromatography mass

spectrometry; LSD: Least significant difference; Mn: Manganese; MRM: Multiple reaction monitoring; MWDB: MetWare database; OPLS-DA: Orthogonal projection to latent structure-discriminant analysis; PAE: Phosphorus acquisition efficiency; PAL: Phenylalanine ammonia; PAP: Purple acid phosphatase; PC1: Principal component one; PCho: Phosphocholine; PGPR: Plant growth-promoting rhizobacteria; PHO2: A ubiquitin-conjugating E2 enzyme; PHR1: phosphate starvation response 1; Pi: Soluble inorganic phosphate; P: Phosphorus; PPi: Inorganic pyrophosphate; PSR: Soluble inorganic phosphate starvation response; PUE: Phosphorus utilization efficiency; QQQ: Triple quadrupole; qRT-PCR: Quantitative real-time polymerase chain reaction; RNS: Ribonuclease; SPX: SYG1/PHO81/XPR1; Stylo: Stylosanthes spp.; T-AOC: Total antioxidant capacity. PCA: Principal component analysis; TPTZ: Tripyridine triacridine; UGT: Uridine diphosphate glycosyltransferase; UPLC: Ultra Performance Liquid Chromatography; VIP: Variable importance in project; VPE: Vacuolar Pi efflux transporter.

Declarations

Ethics approval and consent to participate

Not applicable.

Consent for publication

Not applicable.

Availability of data and material

The datasets are included in this article to support the conclusions and the additional files are also available, the nucleic acid sequence of genes have been submitted to the NCBI database (https://www.ncbi.nlm.nih.gov/) via BankIt repository with the sequence identifier displayed in Additional file 2: Table S1.

Competing of interests

The authors declare no competing interests.

Funding

The research was financially supported by the Natural Science Foundation of Hainan Province (318QN265), the National Natural Science Foundation of China (31701492, 31861143013, 31672483), the Modern Agro-industry Technology Research System (CARS-34, CARS-22-Z11), and the Central Public-interest Scientific Institution Basal Research Fund for CATAS (1630032018004). The authors declare that none of the funding bodies have any role in the design of the study or collection, analysis, interpretation of data and writing the manuscript.

Authors' contributions

P.L. and L.L conceived and designed the study. J.L., Y.L. and J.W. performed the physiological experiments. J.L. and J.W. carried out the metabolic and qRT-PCR analysis. P.L. and J.W. analyzed the data. J.L. wrote the draft manuscript. P.L., G.L., L.L. and Z.C. provided many critical suggestions to revise the manuscript. All authors read and approved the final manuscript.

Acknowledgments

The authors sincerely thank MetWare Biotechnology Limited Company (Wuhan, China) for helping to identify the metabolites.

References

1. Plaxton WC, Lambers H. Phosphorus: back to the roots. In: Lambers H, Plaxton WC, editors. Annual Plant Reviews, Volume 48: Phosphorus metabolism in plants. Hoboken, NJ: John Wiley & Sons; 2015. p. 3-22.
2. Vance CP, Uhde-Stone C, Allan DL. Phosphorus acquisition and use: critical adaptations by plants for securing a nonrenewable resource. New Phytol. 2003;157:423-447.
3. Zhu J, Li M, Whelan M. Phosphorus activators contribute to legacy phosphorus availability in agricultural soils: a review. Sci Total Environ. 2018;612:522-537.
4. López-Arredondo DL, Leyva-González MA, González-Morales SI, López-Bucio J, Herrera-Estrella L. Phosphate nutrition: improving low-phosphate tolerance in crops. Annu Rev Plant Biol. 2014;65:95-123.
5. Gilbert N. Environment: the disappearing nutrient. Nature. 2009;461:716-718.
6. Veneklaas EJ, Lambers H, Bragg J, et al. Opportunities for improving phosphorus-use efficiency in crop plants. New Phytol. 2012;195:306-320.
7. Ha S, Tran LS. Understanding plant responses to phosphorus starvation for improvement of plant tolerance to phosphorus deficiency by biotechnological approaches. Crit Rev Biotechnol. 2014;34:16-30.
8. Liang C, Wang J, Zhao J, Tian J, Liao H. 2014. Control of phosphate homeostasis through gene regulation in crops. Curr Opin Plant Biol. 2014;21:59-66.
9. Lynch JP. Root phenotypes for improved nutrient capture: an underexploited opportunity for global agriculture. New Phytol. 2019;223:548-564.
10. Lin ZH, Chen LS, Chen RB, Zhang FZ, Jiang HX, Tang N, Smith BR. Root release and metabolism of organic acids in tea plants in response to phosphorus supply. J Plant Physiol. 2011;168:644-652.
11. Tran HT, Hurley BA, Plaxton WC. Feeding hungry plants: the role of purple acid phosphatases in phosphate nutrition. Plant Sci. 2010;179:14-27.
12. Roch GV, Marharajan T, Ceasar SA, Ignacimuthu S. The role of PHT1 family transporters in the acquisition and redistribution of phosphorus in plants. Crit Rev Plant Sci. 2019;38:171-198.

13. Raven JA, Lambers H, Smith SE, Westoby M. Costs of acquiring phosphorus by vascular land plants: patterns and implications for plant coexistence. New Phytol. 2018;217:1420-1427.
14. Nakamura Y. Phosphate starvation and membrane lipid remodeling in seed plants. Prog Lipid Res. 2013;52:43-50.
15. Yang SY, Huang TK, Kuo HF, Chiou TJ. Role of vacuoles in phosphorus storage and J Exp Bot. 2017;68:3045-3055.
16. Plaxton WC, Tran HT. Metabolic adaptations of phosphate-starved plants. Plant Physiolo. 2011;156:1006-1015.
17. Chiou TJ, Lin SI. Signaling network in sensing phosphate availability in plants. Annu Rev Plant Biol. 2011;62:185-206.
18. Ham BK, Chen J, Yan Y, Lucas WJ. Insights into plant phosphate sensing and signaling. Curr Opin Biotechnol. 2018;49:1-9.
19. Pant BD, Buhtz A, Kehr J, Scheible WF. MicroRNA399 is a long-distance signal for the regulation of plant phosphate homeostasis. Plant J. 2008;53:731-738.
20. Wang ZY, Hu H, Huang HJ, Duan K, Wu ZC, Wu P. Regulation of *OsSPX1* and *OsSPX3* on expression of *OsSPX* domain genes and Pi-starvation signaling in rice. J Integr Plant Biol. 2009;51(7):663-674.
21. Wang F, Deng MJ, Xu JM, Zhu XL, Mao CZ. Molecular mechanisms of phosphate transport and signaling in higher plants. Semin Cell Dev Biol. 2018;74:114-122.
22. Lin ZH, Chen LS, Chen RB, Zhang FZ, Yang LT, Tang N. Expression of genes for two phosphofructokinases, tonoplast ATPase subunit A, and pyrophosphatase of tea roots in response to phosphorus-deficiency. J Horti Sci Biotech. 2010;85:449-453.
23. Zhang Z, Liao H, Lucas WJ. Molecular mechanisms underlying phosphate sensing, signaling, and adaptation in plants. J Integr Plant Biol. 2014;56:192-220.
24. Lan P, Li W, Schmidt W. Complementary proteome and transcriptome profiling in phosphate-deficient *Arabidopsis* roots reveals multiple levels of gene regulation. Mol Cell Proteomics. 2012;11:1156-1166.
25. Secco D, Jabnoune M, Walker H, Shou H, Wu P, Poirier Y, Whelan J. Spatio-temporal transcript profiling of rice roots and shoots in response to phosphate starvation and recovery. Plant Cell. 2013;25:4285-4304.
26. Torabi S, Wissuwa M, Heidari M, Naghavi MR, Gilany K, Hajirezaei MR, Omidi M, Yazdi-Samadi B, Ismail AM, Salekdeh GH. A comparative proteome approach to decipher the mechanism of rice adaptation to phosphorous deficiency. Proteomics. 2009;9:159-170.
27. Li KP, Xu CZ, Li ZX, Zhang KW. Comparative proteome analyses of phosphorus responses in maize (*Zea mays*) roots of wild-type and a low-P-tolerant mutant reveal root characteristics associated with phosphorus efficiency. Plant J. 2008;55:927-939.
28. Du Q, Wang K, Xu C, Zou C, Xie C, Xu Y, Li W. Strand-specific RNA-Seq transcriptome analysis of genotypes with and without low-phosphorus tolerance provides novel insights into phosphorus-use

efficiency in maize. BMC Plant Biol. 2016;16:222-234.

29. Sun Y, Mu C, Chen Y, et al. Comparative transcript profiling of maize inbreds in response to long-term phosphorus deficiency stress. Plant Physiol Bioch. 2016;109:467-481.
30. Fan F, Cui B, Zhang T, Qiao G, Ding G, Wen X. The temporal transcriptomic Response of *Pinus massoniana* seedlings to phosphorus deficiency. Plos One. 2014;9:e105068.
31. Fan F, Ding G, Wen X. Proteomic analyses provide new insights into the responses of *Pinus massoniana* seedlings to phosphorus deficiency. Proteomics. 2015;16:504-515.
32. Plaxton WC, Lambers H. 'Omics' approaches towards understanding plant phosphorus acquisition and use. In: Lan P, Li W, Schmidt W, editors. Annual Plant Reviews, Volume 48: Phosphorus metabolism in plants. Hoboken, NJ: John Wiley & Sons; 2015. p. 65-97.
33. Sampedro J, Cosgrove DJ. The expansin superfamily. Genome Biol. 2005;6:242-254.
34. Kong Y, Wang B, Du H, Li W, Li X, Zhang C. *GmEXLB1*, a soybean expansin-like B gene, alters root architecture to Improve phosphorus acquisition in Arabidopsis. Front Plant Sci. 2019;10:808-820.
35. Xu L, Zha H, Wan R, et al. Identification of vacuolar phosphate efflux transporters in land plants. Nat Plants. 2019;5:84-94.
36. Plaxton WC, Lambers H. Metabolomics of plant phosphorus-starvation response. In: Jones C, Hatier JH, Cao M, Fraser K, Rasmussen S, editors. Annual Plant Review, Volume 48: Phosphorus metabolism in plants. Hoboken, NJ: John Wiley & Sons; 2015. p. 217-236.
37. Pant BD, Pant P, Erban A, Huhman D, Kopka J, Scheible WR. Identification of primary and secondary metabolites with phosphorus status-dependent abundance in Arabidopsis, and of the transcription factor PHR1 as a major regulator of metabolic changes during phosphorus limitation. Plant Cell Environ. 2015;38:172-187.
38. Tawaraya K, Horie R, Wagatsuma T, Saito K, Oikawa A. Metabolite profiling of shoot extract, root extract, and root exudate of rice under nitrogen and phosphorus deficiency. Soil Sci Plant Nutr. 2018;64:1-11.
39. Ganie AH, Ahmad A, Pandey R, Aref IM, Yousuf PY, Ahmad S, Iqbal M. Metabolite profiling of low-P tolerant and low-P sensitive maize genotypes under phosphorus starvation and restoration conditions. Plos One. 2015;10:e0129520.
40. Huang CY, Roessner U, Eickmeier I, Genc Y, Callahan DL, Shirley N, Langridge P, Bacic A. Metabolite profiling reveals distinct changes in carbon and nitrogen metabolism in phosphate-deficient barley plants (*Hordeum vulgare*). Plant Cell Physiol. 2008;49:691-703.
41. Nguyen VL, Palmer L, Roessner U, Stangoulis J. Genotypic variation in the root and shoot metabolite profiles of wheat (*Triticum aestivum*) indicate sustained, preferential carbon allocation as a potential mechanism in phosphorus efficiency. Front Plant Sci. 2019;10:995-1009.
42. Mo X, Zhang M, Liang C, Cai L, Tian J. Integration of metabolome and transcriptome analyses highlights soybean roots responding to phosphorus deficiency by modulating phosphorylated metabolite processes. Plant Physiol and Bioch. 2019;139:697-706.

43. Kc S, Liu M, Zhang Q, Fan K, Shi Y, Ruan J. Metabolic changes of amino acids and flavonoids in tea plants in response to inorganic phosphate limitation. Int J Mol Sci. 2018;19:3683- 3704.
44. Weston LA, Mathesius U. Flavonoids: their structure, biosynthesis and role in the rhizosphere, including allelopathy. J Chem Ecol. 2013;39:283-297.
45. Marques A, Moraes L, Aparecida Dos Santos M, et al. Origin and parental genome characterization of the allotetraploid *Stylosanthes scabra* Vogel (Papilionoideae, Leguminosae), an important legume pasture crop. Ann Bot. 2018;122:1143-1159.
46. Kochian LV, Hoekenga OA, Pineros MA. How do crop plants tolerate acid soils? Mechanisms of aluminum tolerance and phosphorous efficiency. Annu Rev Plant Biol. 2004;55:459-493.
47. Jiang C, Liu L, Li X, Han R, Wei Y, Yu Y. Insights into aluminum-tolerance pathways in *Stylosanthes* as revealed by RNA-Seq analysis. Sci Rep. 2018;8:6072-6081.
48. Liu P, Huang R, Hu X, Jia Y, Li J, Luo J, Liu Q, Luo L, Liu G, Chen Z. Physiological responses and proteomic changes reveal insights into *Stylosanthes* response to manganese toxicity. BMC Plant Biol. 2019;19:212-233.
49. Sun F, Suen PK, Zhang Y, Liang C, Carrie C, Whelan J, Ward JL, Hawkins ND, Jiang L, Lim BL. A dual-targeted purple acid phosphatase in *Arabidopsis thaliana* moderates carbon metabolism and its overexpression leads to faster plant growth and higher seed yield. New Phytol. 2012;194:206-219.
50. Kaashyap M, Ford R, Kudapa H, Jain M, Edwards D, Varshney R, Mantri N. Differential regulation of genes involved in root morphogenesis and cell wall modification is associated with salinity tolerance in chickpea. Sci Rep. 2018;8:4855-4874.
51. Motte H, Vanneste S, Beeckman T. Molecular and environmental regulation of root development. Annu Rev Plant Biol. 2019;70:465-488.
52. Cosgrove DJ. Plant expansins: diversity and interactions with plant cell walls. Curr Opin Plant Biol. 2015;25:162-172.
53. Han YY, Zhou S, Chen YH, Kong X, Xu Y, Wang W. The involvement of expansins in responses to phosphorus availability in wheat, and its potentials in improving phosphorus efficiency of plants. Plant Physiol Biochem. 2014;78:53-62.
54. Guo W, Zhao J, Li X, Qin L, Yan X, Liao H. A soybean β-expansin gene *GmEXPB2* intrinsically involved in root system architecture responses to abiotic stresses. Plant J. 2011;66:541-552.
55. Plaxton WC, Lambers H. Sensing, signaling and control of phosphate starvation in plants: molecular players and application. In: Scheible WR, Rojas-Triana M, editors. Annual Plant Reviews, Volume 48: Phosphorus metabolism in plants. Hoboken, NJ: John Wiley & Sons; 2015. p. 23-63.
56. Byrne SL, Foito A, Hedley PE, Morris JA, Stewart D, Barth S. Early response mechanisms of perennial ryegrass (*Lolium perenne*) to phosphorus deficiency. Ann Bot. 2011;107:243-254.
57. Ruan YL. Sucrose metabolism: gateway to diverse carbon use and sugar signaling. Annu Rev Plant Biol. 2014;65:33-67.

58. Sami F, Siddiqui H, Hayat S. Interaction of glucose and phytohormone signaling in plants. Plant Physiol and bioch. 2019;135:119-126.
59. Dissanayaka DMSB, Plaxton WC, Lambers H, Siebers M, Marambe B, Wasaki J. Molecular mechanisms underpinning phosphorus-use efficiency in rice. Plant Cell Environ. 2018;41:1483-1496.
60. Müller J, Gödde V, Niehaus K, Zörb C. Metabolic adaptations of white lupin roots and shoots under phosphorus deficiency. Front Plant Sci. 2015;6:1014-1024.
61. Zhang S, Tang D, Korpelainen H, Li C. Metabolic and physiological analyses reveal that *Populus cathayana* males adopt an energy-saving strategy to cope with phosphorus deficiency. Tree Physiol. 2019;39:1630-1645.
62. Hassan S, Mathesius U. The role of flavonoids in root-rhizosphere signalling: opportunities and challenges for improving plant-microbe interactions. J Exp Bot. 2012;63(9):3429-3444.
63. Stewart AJ, Chapman W, Jenkins GI, Graham IA, Martin T, Crozier A. The effect of nitrogen and phosphorus deficiency on flavonol accumulation in plant tissues. Plant Cell Environ. 2001;24:1189-1197.
64. Ishimaru Y, Kakei Y, Shimo H, Bashir K, SatoY, Sato Y, Uozumi N, Nakanishi H, Nishizawa NK. A rice phenolic efflux transporter is essential for solubilizing precipitated apoplasmic iron in the plant stele. J Biol Chem. 2011;286:24649-55.
65. Malusà E, Russo MA, Monterumici CM, Belligno A. Modification of secondary metabolism and flavonoid biosynthesis under phosphate deficiency in bean roots. J Plant Nutr. 2006;29:245-258.
66. Juszczuk I, Wiktorowska A, Malusá, Rychter AM. Changes in the concentration of phenolic compounds and exudation induced by phosphate deficiency in bean plants (*Phaseolus vulgaris*). Plant Soil. 2004;267:41-49.
67. Hu H, Tang C, Rengel Z. Role of phenolics and organic acids in phosphorus mobilization in calcareous and acidic soils. J Plant Nutr. 2005;28:1427-1439.
68. Scagel CF. Phenolic composition of basil plants is differentially altered by plant nutrient status and inoculation with mycorrhizal fungi. Hortscience. 2012;47:660-671.
69. Bassard JE, Ullmann P, Bernier F, Werck-Reichhart D. Phenolamides: bridging polyamines to the phenolic metabolism. Phytochemistry. 2010;71:1808-1824.
70. Valette M, Rey M, Gerin F, Comte G, Wisniewski-Dyé F. A common metabolomic signature is observed upon inoculation of rice roots with various rhizobacteria. J Integr Plant Biol. 2019.
71. Famoso AN, Clark RT, Shaff JE, Craft E, McCouch SR, Kochian LV. Development of a novel aluminum tolerance phenotyping platform used for comparisons of cereal aluminum tolerance and investigations into rice aluminum tolerance mechanisms. Plant Physiol. 2010;153:1678-1691.
72. Murphy J, Riley JP. A modified single solution method for the determination of phosphate in natural waters. Analytica Chimica Acta. 1962;27:31-36.
73. Liu PD, Xue YB, Chen ZJ, Liu GD, Tian J. Characterization of purple acid phosphatases involved in extracellular dNTP utilization in *Stylosanthes*. J Exp Bot. 2016;67:4141-4154.

74. Qiao D, Ke C, Hu B, Luo JG, Ye H, Sun Y, Yan XY, Zeng XX. Antioxidant activities of polysaccharides from *Hyriopsis cumingii*. Carbohyd Polym. 2009;78:199-204.
75. Bradford MM. A rapid and sensitive method for the quantitation of microgram quantities of protein utilizing the principle of protein-dye binding. Anal Biochem. 1976;72:248-254.
76. Chen W, Gong L, Guo Z, Wang W, Zhang H, Liu X, Yu S, Xiong L, Luo J. A novel integrated method for large-scale detection, identification, and quantification of widely targeted metabolites: application in the study of rice metabolomics. Mol Plant. 2013;6:1769-1780.
77. Fraga CG, Clowers BH, Moore RJ, Zink EM. Signature-discovery approach for sample matching of a nerve-agent precursor using liquid chromatography-mass spectrometry, XCMS, and chemometrics. Anal Chem. 2010;82:4165-4173.
78. Thévenot EA, Roux A, Xu Y, Ezan E, Junot C. Analysis of the human adult urinary metabolome variations with age, body mass index, and gender by implementing a comprehensive workflow for univariate and OPLS statistical analyses. J Proteome Res. 2015;14:3322-35.
79. Liu PD, Cai ZF, Chen ZJ, Mo XH, Ding XP, Liang CY, Liu GD, Tian J. A root-associated purple acid phosphatase, SgPAP23, mediates extracellular phytate-P utilization in *Stylosanthes guianensis*. Plant Cell Environ. 2018;41:2821-2834.
80. Zhang QF, Liu M, Ruan JY. Metabolomics analysis reveals the metabolic and functional roles of flavonoids in light-sensitive tea leaves. BMC Plant Biol. 2017;17:64-74.

Additional Files

Additional file 1: Fig. S1 Growth performance of stylo at two P levels. Plants were grown in hydroponics for 15 d with (+Pi) or without (-Pi) 250 μmol/L KH_2PO_4 addition. Each bottle contained six plants. (DOCX 1.86 MB)

Additional file 1: Fig. S2 Effects of Pi availability on the ratio of root increase. (a) Total root length. (b) Root surface area. (c) Root volume. After precultured under +Pi (250 μmol/L K_2HPO_4) for 7 d, stylo seedlings were transferred into nutrient solution with (+Pi) or without (-Pi) 250 μmol/L KH_2PO_4 additions for 7, 10, 15, 20 d. Each bar represents the mean of four replicates with SE (n = 6). Different lowercase letters indicate significant difference among groups ($P < 0.05$). Ratio of increased under -Pi (%) = [(-Pi - +Pi)/+Pi] * 100. (DOCX 1.86 MB)

Additional file 1: Fig. S3 Ratio of root/shoot in stylo at two P treatments. Uniform 7-d old stylo seedling were transferred into nutrient solution with (+Pi) or without (-Pi) 250 μmol/L KH_2PO_4 additions for 15 d. Asterisks represent significant differences between +Pi and -Pi treatments. * $P \leq 0.05$, ** $P \leq 0.01$, *** $P \leq 0.001$. (DOCX 1.86 MB)

Additional file 1: Fig. S4 Physiological and biochemical levels in response to low P stress in stylo roots. (a) Total P concentration of shoot and root; (b) APase activity; (c) PAL activity; (d) total phenol content; (e) flavonoid content; (f) T-AOC activity. Stylo seedlings were precultured in hydroponics for 7 d with 250

μmol/L KH_2PO_4 and subsequently transferred into nutrient solution with (+Pi) or without (-Pi) 250 μmol/L KH_2PO_4 additions for 15 d. Each bar represents the mean of four replicates with SE (n = 3 or 4). Asterisks represent significant differences between +Pi and -Pi treatments. * $P \leq 0.05$, ** $P \leq 0.01$. P: phosphate, APase: acid phosphatase, T-AOC: total antioxidant capacity, PAL: phenylalanine ammonia lyase, DW: dry weight, FW: fresh weight. (DOCX 1.86 MB)

Additional file 1: Fig. S5 Phylogenetic analysis of stylo expansin proteins with other expansin proteins in plants. At: *Arabidopsis thaliana*; Gm: *Glycine max*; Ta: *Triticum aestivum*; Sg: *Stylosanthes guianensis*. EXPA: α-expansin; EXLA: expansin-like A; EXPB: β-expansin; EXLB: expansin-like B. (DOCX 1.86 MB)

Additional file 1: Fig. S6 Clustered heatmap of differentially accumulated metabolites (DAMs) in stylo roots at low P stress. Individual metabolites are represented by rows and nutritional status are represented by columns. Heatmap visualization of metabolites is based on standardized transformation (Z score) of metabolite concentrations. (DOCX 1.86 MB)

Additional file 1: Fig. S7 Expression analysis of *SgPAPs* and *SgRNSs* genes in response to Pi starvation. Expression of five *SgPAPs* and four *SgRNSs* in stylo roots exposed to +Pi (250 μmol/L KH2PO4) or -Pi (no KH2PO4 added) treatments for 15 d. Each bar represents the mean of four replicates with SE (n = 4) Asterisks indicate significant differences between +Pi and -Pi treatments. * $P \leq 0.05$, ** $P \leq 0.01$, *** $P \leq 0.001$. ns indicates no significant difference. (DOCX 1.86 MB)

Additional file 2: Table S1 A list of primers used for qRT-PCR and gene accession numbers in NCBI database. (DOCX 25.5 kb)

Additional file 3: Table S2 General information of identified metabolites from metabolomic analysis in stylo roots. (XLSX 75.0 kb)

Additional file 4: Table S3 General information about differentially accumulated metabolites (DAMs) from metabolomic analysis in stylo roots. (XLSX 49.3 kb)

Figures

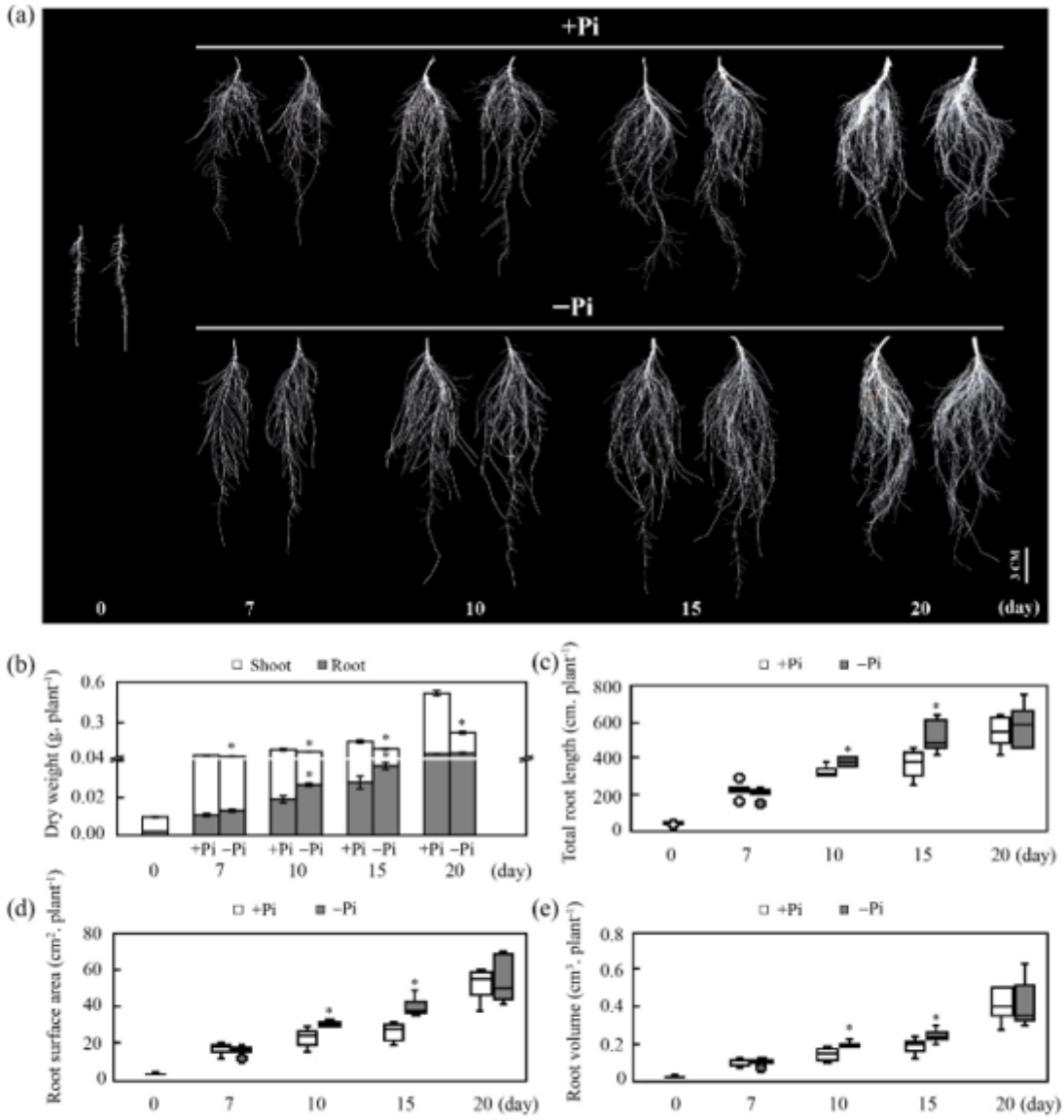

Figure 1

Effects of Pi availability on stylo growth. (a) Root growth performance; (b) dry weight of shoots and roots; (c) total root length; (d) root surface area; (d) root volume. Uniform 7d-old stylo seedlings were transferred into nutrient solution with (+Pi) or without (−Pi) 250 μmol/L KH2PO4 additions for 0, 7, 10, 15 or 20 d growth. Quartile (box), maximum and minimum (whiskers) and outlying values (circles) are shown in boxplots. Six biological replicates are contained in each experimental group (n = 6). Error bars indicate standard error (SE). Asterisks represent significant differences between +Pi and −Pi treatments ($P < 0.05$). Bar = 3 cm.

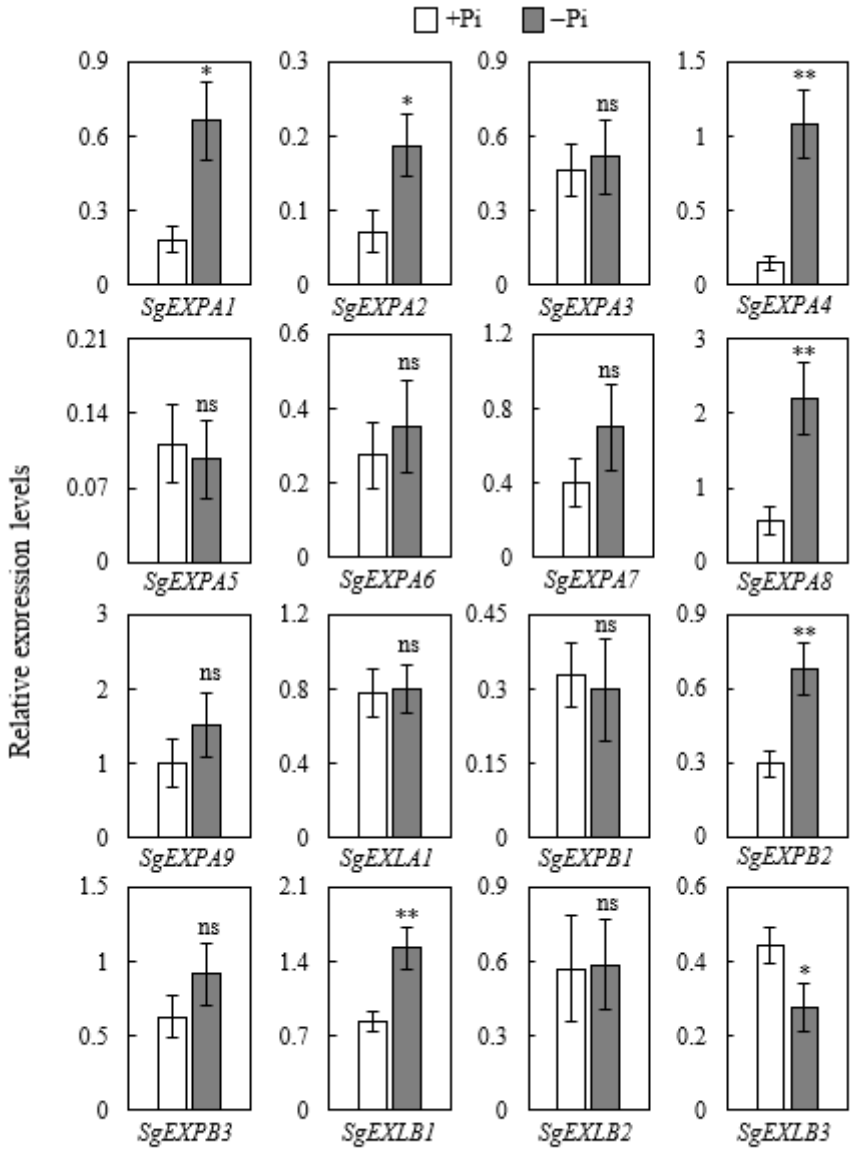

Figure 2

Expression analysis of genes encoding expansin proteins at two P levels. Stylo seedlings were exposed to +Pi (250 μmol/L KH2PO4) and −Pi (0 μmol/L KH2PO4) treatments for 15 d. The roots were harvested for qRT-PCR analysis. Each bar represents the mean of four replicates with SE (n = 4). Asterisks indicate significant differences between +Pi and −Pi treatments. * $P \leq 0.05$, ** $P \leq 0.01$. ns indicates no significant difference.

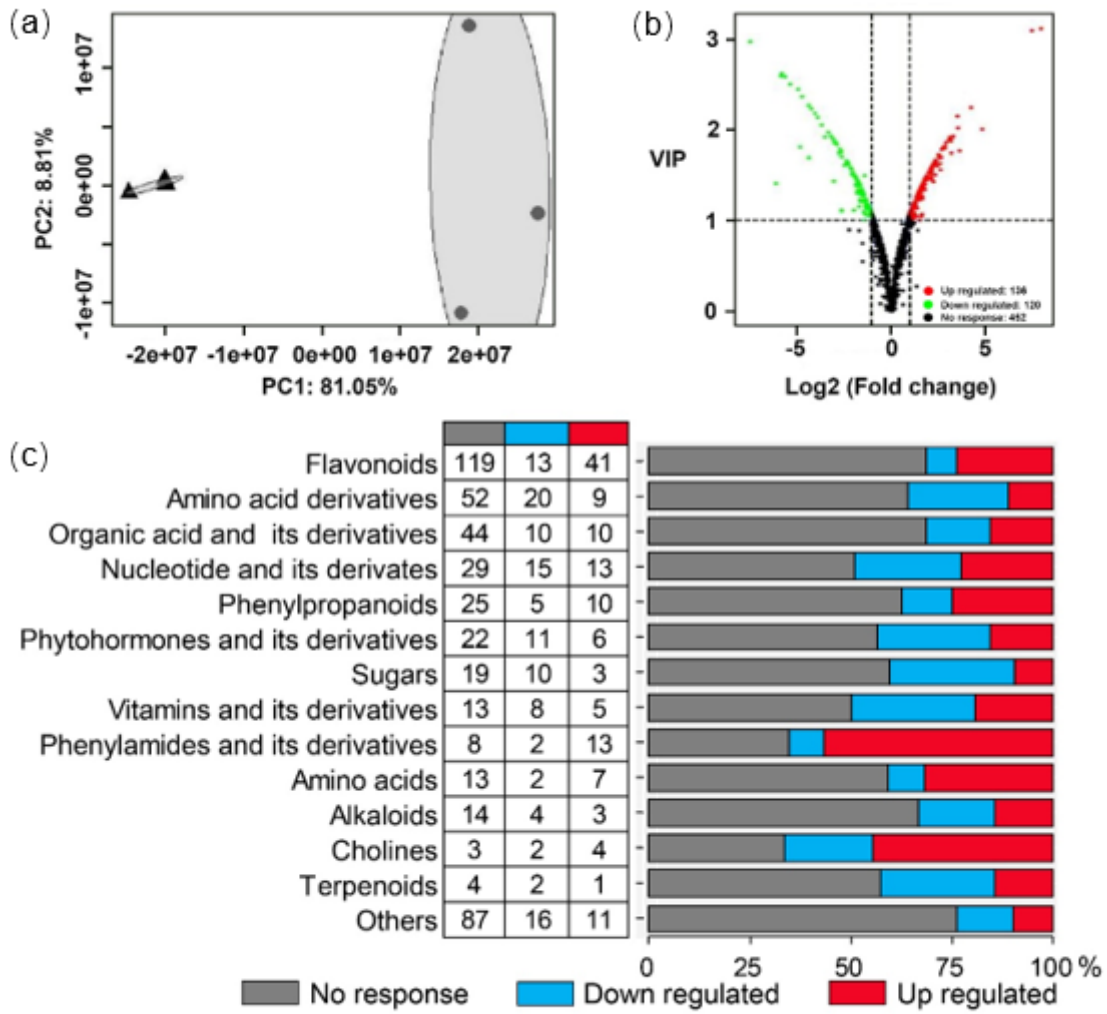

Figure 3

Overview of metabolomic changes in stylo roots at two P treatments. (a) Principal component (PC) scores of metabolic the first two variances in stylo roots (n = 3). Stylo seedlings were grown in +Pi (250 μmol/L KH2PO4, triangles) and −Pi (0 μmol/L KH2PO4, circles) nutrient solutions for 15 d. The confidence level in the grey confidence circle is 95%. (b) The volcano diagram of distribution metabolites in stylo roots response to P deficiency. Red circles, green circles and black circles indicate up regulated, down regulated and no response metabolites, respectively. (c) Category of differentially accumulated metabolites (DAMs) in stylo roots during low P stress. Data are shown as the number of metabolites, DAMs are defined by conforming the variable importance in project (VIP) ≥ 1.0 and −Pi/+Pi ≥ 2.0 or ≤ 0.5. Up-regulated: −Pi/+Pi ≥ 2.0, down-regulated: −Pi/+Pi ≤ 0.5.

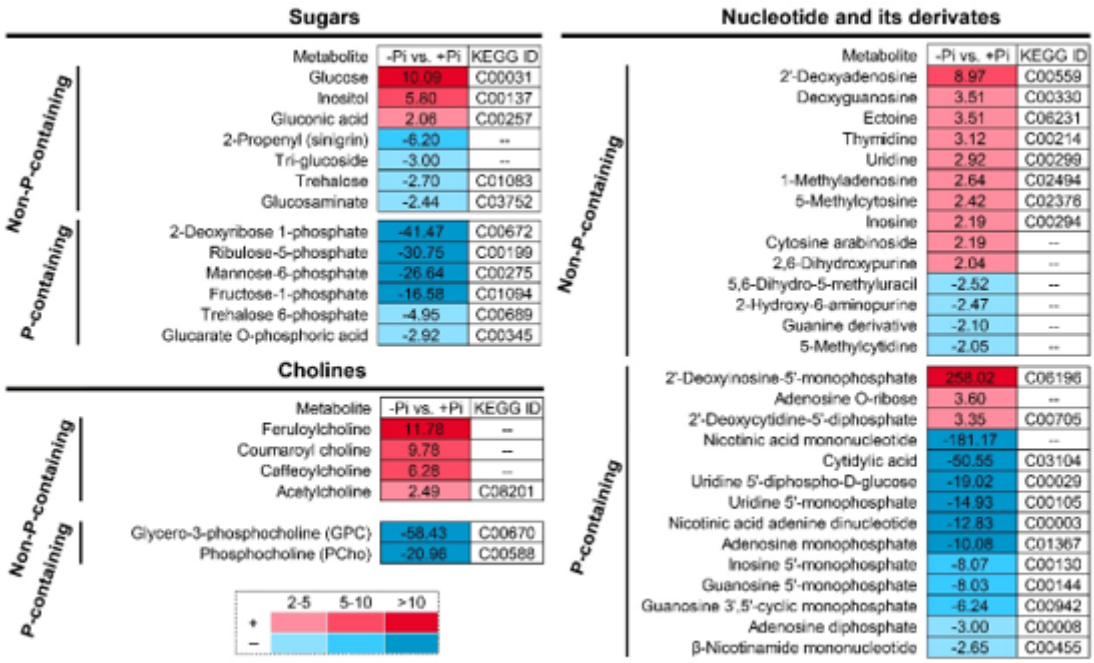

Figure 4

Effects of Pi availability on the relative levels of sugars, cholines, nucleotide and its derivatives in stylo roots. Data are shown as heatmap for the response ratio of Pi (0 μmol/L KH2PO4) relative to +Pi (250 μmol/L KH2PO4) (n = 3). Response ratios are shown as positive numbers for an increase or negative inverted number for a decrease. In addition, the column of Kyoto Encyclopedia of Genes and Genomes identity (KEGG ID) is obtained from KEGG database (https://www.kegg.jp/). "–" in this figure represents the metabolite without an ID in KEGG database.

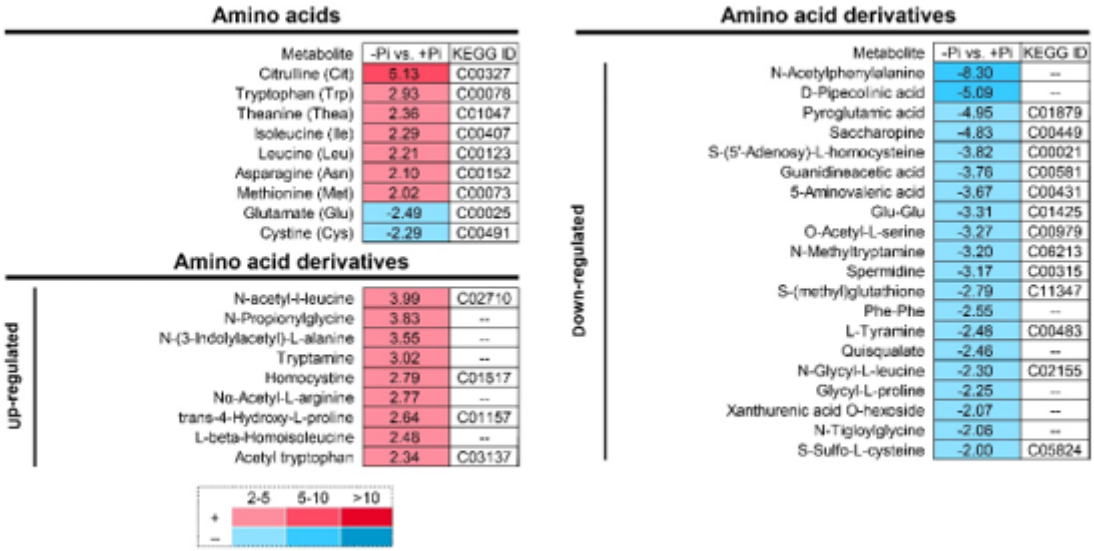

Figure 5

Alternations in amino acid and its derivatives in stylo roots response to Pi starvation. Data indicate the response ratio of −Pi (0 μmol/L KH2PO4) relative to +Pi (250 μmol/L KH2PO4) (n = 3). in heatmap. Positive numbers and negative inverted numbers represent an increase and decrease in response to P deficiency, respectively. KEGG IDs are obtained from KEGG database (https://www.kegg.jp/). "–" in this figure represents the metabolite without an ID in KEGG database.

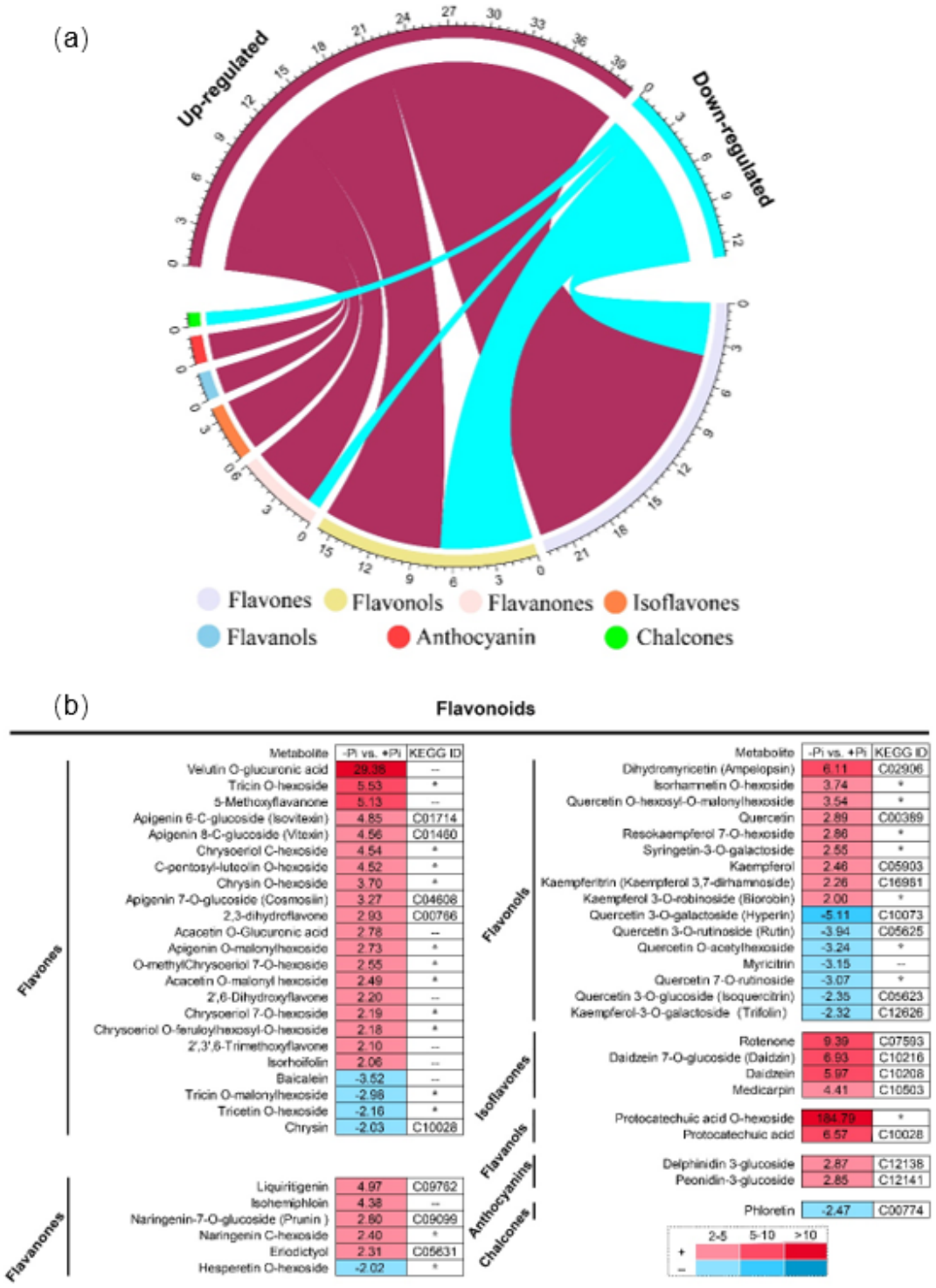

Figure 6

Analysis of flavonoid metabolites in stylo roots at low P stress. (a) Circle graph of seven subcategory flavonoid metabolites. Digital scale represents the number of corresponding metabolites. Up-regulated or down-regulated metabolites were screened according to the criterion of fold changes ≥ 2.0 or ≤ 0.5, and VIP ≥1.0 (n = 3). (b) Heatmap of flavonoid metabolites. Fold changes of metabolites (−Pi/+Pi) are shown as numbers, and the ratio of −Pi/+Pi less than 0.5 is inverted as negative a number (n = 3). The metabolite ID of KEGG database was listed in the last column, "–" and "*" indicate the metabolites without an ID in KEGG database, and "*" represents a glycoside derivative.

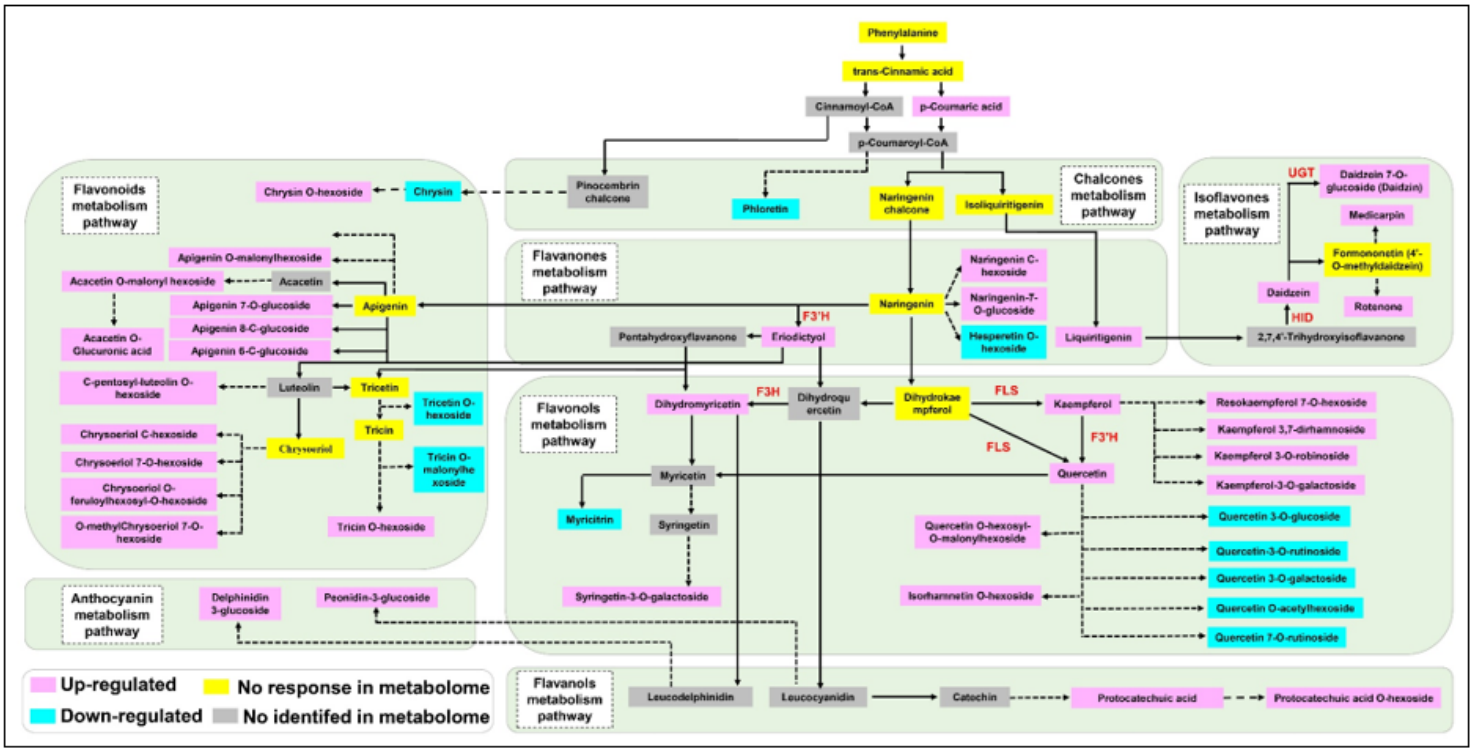

Figure 7

Flavonoid metabolism pathway in stylo roots response to P deficiency. The pathway was designed based on KEGG pathways (http://www.kegg.jp/kegg/pathway.html) and researches described by Zhang et al. [80] and Kc et al. [43]. The light red, blue, yellow and grey colors indicate up-regulated, down-regulated, no response and no identified metabolites in metabolome, respectively. The solid arrows show direct and dotted arrows represent indirect and speculated steps in the pathway. Vital genes are marked on the metabolic procedure.

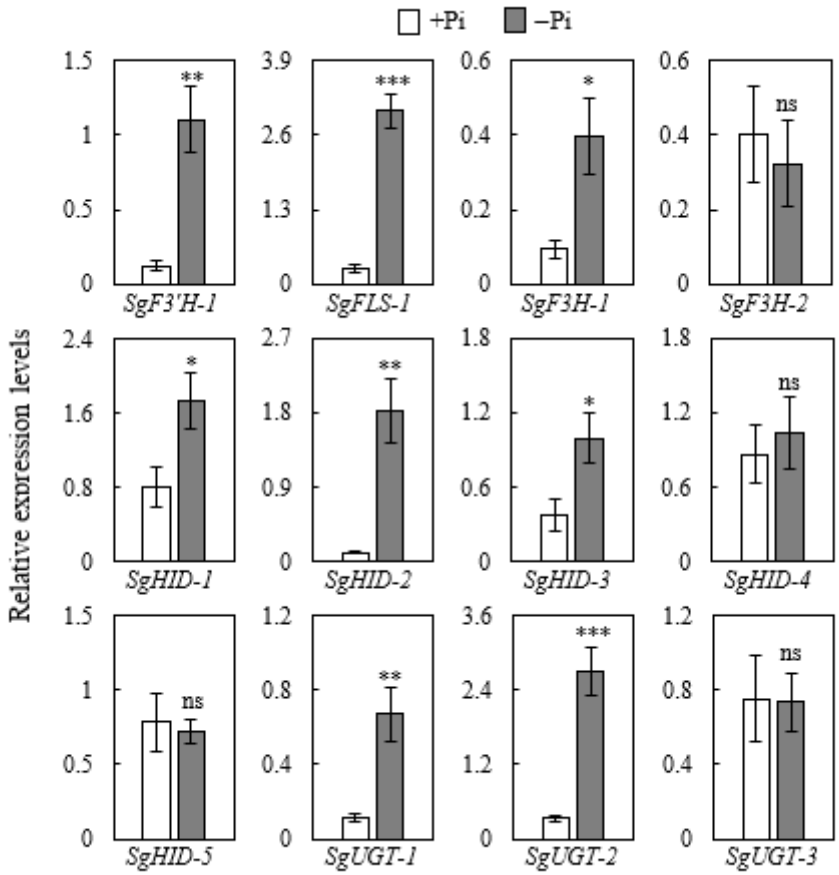

Figure 8

Expression analysis of candidate key genes associated with flavonoid metabolism in stylo roots at low P stress. The expression of 12 genes were analyzed in roots of stylo at +Pi and −Pi treatments for 15 d. Transcript expression levels were normalized using housekeeping gene SgEF1α. Each bar represents the mean of four replicates with SE (n = 4). Asterisks indicate significant differences between +Pi and −Pi treatments. * P ≤ 0.05, ** P ≤ 0.01, *** P ≤ 0.001. ns indicates no significant difference.

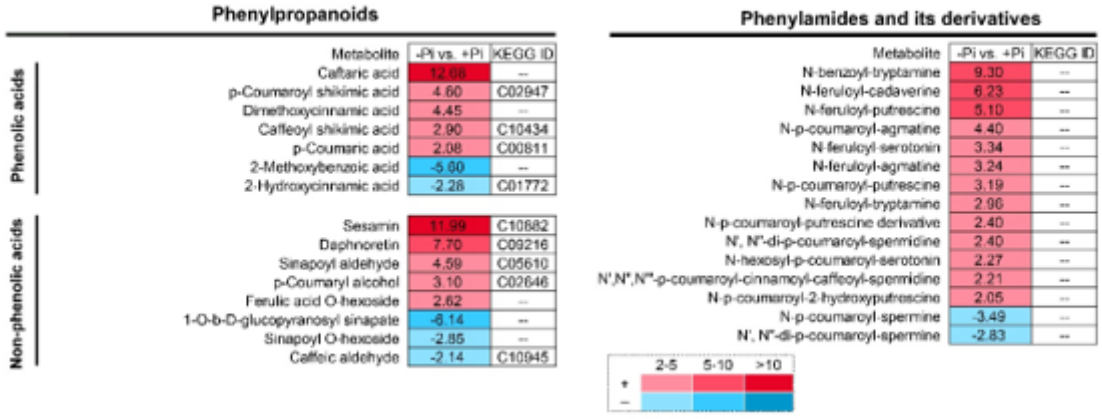

Figure 9

Changes in phenylpropanoids, phenylamides and its derivatives in stylo roots response to low P stress. Numbers indicate the fold changes, and negative numbers represent the inverted fold changes less than 0.5 (Pi/+Pi < 0.5). KEGG ID of metabolites were displayed in the last column. "–" indicate the metabolites without an ID in KEGG database.

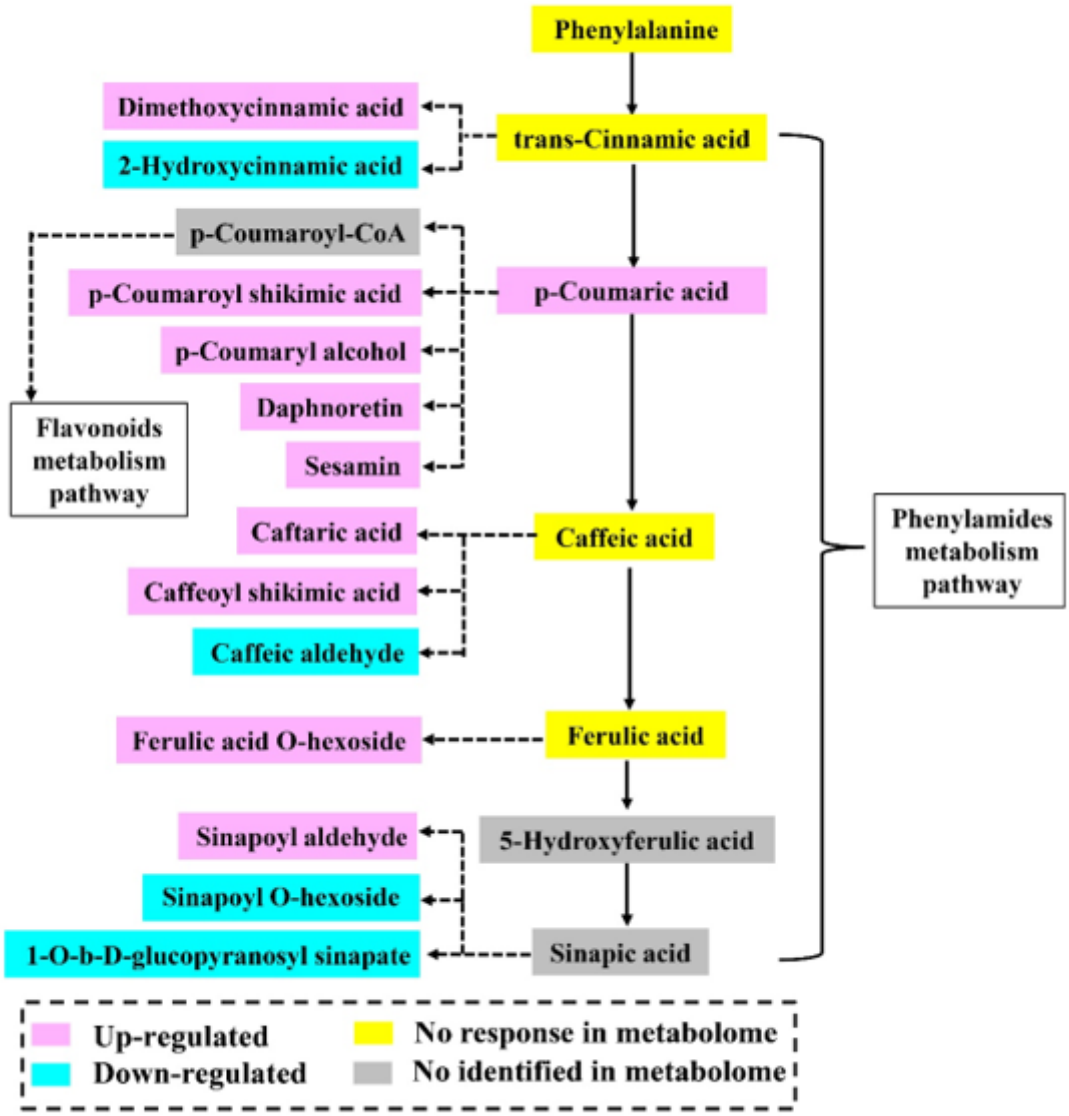

Figure 10

Phenylpropanoids metabolism pathway in stylo roots response to low P stress. The pathway was designed based on KEGG pathway database. The light red, blue, yellow and grey colors indicate up-regulated, down-regulated, no response and no identified metabolites in metabolome, respectively. The solid arrows show direct steps in the pathway, whereas dotted arrows represent indirect and speculated steps in the pathway.

Supplementary Files

This is a list of supplementary files associated with this preprint. Click to download.

- Additionalfile2TableS1.docx
- Additionalfile1Fig.S1S7.docx
- Additionalfile3TableS2.xlsx
- Additionalfile4TableS3.xlsx